Combining Biomarker and Bulk Compositional Gradient Analysis to Assess Reservoir Connectivity

Andrew E. Pomerantz*[a], G. Todd Ventura[b], Amy M. McKenna[c], Jesús A. Cañas[a], John Auman[d], Kyle Koerner[d], David Curry[d], Robert K. Nelson[b], Christopher M. Reddy[b], Ryan P. Rodgers[c,e], Alan G. Marshall[c,e], Kenneth E. Peters[f], and Oliver C. Mullins[a]

a. Schlumberger-Doll Research, 1 Hampshire St., Cambridge, MA 02139

b. Department of Marine Chemistry and Geochemistry, Woods Hole Oceanographic Institution, Woods Hole, MA 02543

c. Department of Chemistry & Biochemistry, Florida State University, Tallahassee, FL 32306

d. Devon Energy Corporation, 1200 Smith St., Houston, TX 77002

e. National High Magnetic Field Laboratory, Florida State University, 1800 East Paul Dirac Drive, Tallahassee, FL 32310

f. Schlumberger Integrated Services for Exploration, 18 Manzanita Place, Mill Valley, CA 94941

* author to whom correspondence should be addressed: apomerantz@slb.com; telephone +1 617-768-2325, fax +1 617-768-2386

Submitted to Organic Geochemistry (MS #OG-871):	10 July, 2009
Revised manuscript submitted:	20 November, 2009
2nd Revised manuscript submitted:	20 April, 2010

Abstract:

Hydraulic connectivity of petroleum reservoirs represents one of the biggest uncertainties for both oil production and petroleum system studies. Here, a geochemical analysis involving bulk and detailed measures of crude oil composition is shown to constrain connectivity more tightly than is possible with conventional methods. Three crude oils collected from different depths in a single well exhibit large gradients in viscosity, density, and asphaltene content. Crude oil samples are collected with a wireline sampling tool providing samples from well-defined locations and relatively free of contamination by drilling fluids; the known provenance of these samples minimizes uncertainties in the subsequent analysis. The detailed chemical composition of almost the entire crude oil is determined by use of comprehensive two-dimensional gas chromatography (GC×GC) to interrogate the nonpolar fraction and negative ion electrospray ionization Fourier transform ion cyclotron resonance mass spectrometry (ESI FT-ICR MS) to interrogate the polar fraction. The simultaneous presence of 25-norhopanes and mildly altered normal and isoprenoid alkanes is detected, suggesting that the reservoir has experienced multiple charges and contains a mixture of oils biodegraded to different extents. The gradient in asphaltene concentration is explained by an equilibrium model considering only gravitational segregation of asphaltene nanoaggregates; this grading can be responsible for the observed variation in viscosity. Combining these analyses yields a consistent picture of a connected reservoir in which the observed viscosity variation originates from gravitational segregation of asphaltene nanoaggregates in a crude oil with high asphaltene concentration resulting from multiple charges, including one charge that suffered severe biodegradation. Observation of these gradients having appropriate magnitudes suggests good reservoir connectivity with greater confidence than is possible with traditional techniques alone.

Keywords: compositional grading; reservoir connectivity; comprehensive two-dimensional gas chromatography; GC×GC; Fourier transform mass spectrometry; ion cyclotron resonance; FTMS; FT-ICR; electrospray ionization

1. Introduction:

One of the biggest risk factors in oil production is reservoir connectivity—the question of whether a reservoir consists of a single flow unit or a set of compartmentalized flow units separated by sealing barriers. Fundamental reservoir management issues such as the appropriate number of wells to drill depend critically on this important aspect of reservoir architecture. Similarly, geochemical studies of petroleum systems must consider potential compartmentalization. For example, it is now recognized that reservoir fluids are often compositionally graded, with several mechanisms potentially responsible for the grading (Høier and Whitson, 2001; Ratulowski *et al.*, 2003; Stainforth, 2004; Wilhelms and Larter, 2004). Before the composition of reservoir fluids can be used to assess reservoir history and dynamics, reservoir architecture must be understood at least well enough to determine how well the collected oil samples represent fluids from the remainder of the reservoir.

Despite the importance of reservoir connectivity, current methods of assessing connectivity can have large errors (Mullins, 2008). For example, the most common method of assessing connectivity is measuring fluid pressure at various depths in the oil column. If the pressures are continuous with a gradient consistent with the fluid density, the reservoir is assumed to be connected over the interval investigated. However, pressure communication can build up over geologic time through very low permeability and does not guarantee sufficient permeability to permit appreciable flow over production time; pressure communication is a necessary but not sufficient condition for flow connectivity. Petrophysical logs such as gamma-ray measurements detect lithologic changes potentially indicating sealing barriers, but such near-wellbore measurements do not guarantee the aerial extent of the layers throughout the reservoir and do not necessarily have the vertical resolution to detect relevant barriers (Mullins, 2008). Geochemical fingerprinting of oils from different locations in the column is another common method for assessing connectivity. If the fingerprints are similar, the reservoir is assumed to

be connected over the interval sampled. However, oils generated from the same source rock can yield similar fingerprints even if the reservoir is currently compartmentalized and oils from different locations in a connected reservoir can have different composition due to various factors besides compartmentalization. The only proof of reservoir connectivity comes during production, which in deepwater reservoirs occurs after most of the development costs.

This contribution describes the application of a geochemical study and colloidal analysis of asphaltenes to assess reservoir connectivity prior to production. In this example, fluids collected from well-defined depths over a 53 m range in the reservoir are found to have marked gradients in viscosity, asphaltene content, and API gravity. A diverse set of geochemical analyses leads to a consistent picture of a connected reservoir in which the viscosity gradient results from a gradient in asphaltene content in a crude oil that is the commingled product of multiple charges including one biodegraded charge. The analysis constrains connectivity more tightly than is possible with pressure or geochemical fingerprints.

One unique aspect of this study is that it combines bulk and chemically specific methods to analyze the composition of crude oil. The detailed fluid composition is determined by comprehensive two-dimensional gas chromatography (GC×GC) and electrospray ionization Fourier transform-ion cyclotron resonance mass spectrometry (ESI FT-ICR MS). This pair of sophisticated, complementary analytical techniques is capable of determining the detailed composition of almost an entire petroleum sample: GC×GC interrogates the nonpolar fraction and ESI FT-ICR MS interrogates the polar fraction. We note that only negative ion electrospray results are presented here, so only the acidic sub-fraction of the polar fraction is detected; a similar experiment also employing positive ion ESI FT-ICR MS would come closer to the ultimate goal of measuring the entire petroleome (Marshall and Rodgers, 2008). The great detail with which the composition of crude oil can be determined by these high resolution and high accuracy techniques enhances the confidence of the geochemical analysis. Moreover, the relative

abundance of light and heavy ends is determined by optical spectroscopy. Although its resolution is inferior to that of the above techniques, optical spectroscopy provides a bulk analysis that effectively ties together the detailed analyses to provide an even more complete characterization of the composition of crude oil.

2. Geological Context:

Three oil samples were collected from a petroleum reservoir undergoing active development. The oilfield samples were acquired with the Modular Formation Dynamics Tester (MDT, mark of Schlumberger) in an openhole setting, shortly after the well was drilled and prior to casing the oil-bearing zone. The MDT sample acquisition and analysis tool has a probe module for extracting fluid samples from the formation. This probe module (Figure 1) has a stout steel tube (with a concentric flowline) that is pushed firmly against the permeable zone of interest. An onboard pump reduces the flowline pressure causing formation fluids to flow into the tool; sample bottles can then be filled with formation fluids. Downhole fluid analysis (DFA) tools employing optical spectroscopy validate the identity of the fluids in the flowline and can confirm that the fluids are virgin formation fluids (Mullins, 2008). In addition, the DFA tools can be used to quantify compositional variation of crude oils in the reservoir enabling validation of corresponding laboratory results. The sample bottles containing the reservoir fluids are brought to surface, restored to downhole pressures and temperatures at the well site, transferred to transportable sample bottles, and shipped to the laboratory. The exact provenance and identity of the samples analyzed in the laboratory are validated with the complete MDT-DFA log report. The samples are all taken from the same well at the following depths: xx17 m, xx51 m, and xx70 m; the first digits of the depths are obscured to preserve the anonymity of the reservoir and are not essential to the analysis presented here.

Figure 1 near here

The bulk composition and physical properties of the samples are determined by standard analyses and are listed below. The oils gas-oil ratio (GOR) is similar for all samples and is approximately 50 scf/bbl, the saturation pressure is approximately 300 psi, and the reservoir temperature is approximately 65 °C. Figure 2 presents the viscosity (dead oil at room temperature), asphaltene content (asphaltenes are defined operationally as the toluene-soluble, *n*-heptane insoluble fraction), and API gravity for each oil; a gradient in all quantities is apparent. Live oil viscosities are similar to the dead oil viscosities presented here, consistent with the low gas-oil ratio of the live fluids. Viscosity gradients are frequently observed in petroleum reservoirs and can be quite steep or even discontinuous in the vicinity of an oil-water contact, i.e., a tar mat (Head *et al.*, 2003; Hetherington and Horan, 1960). It is common for low GOR black oils to exhibit significant heavy end gradients and almost no GOR gradient (Høier and Whitson, 2001; Mullins, 2008). However, such an extensive gradient occurring over a larger depth range in the reservoir as found here has different and important implications for oil production. Such gradients can arise from biodegradation, charge history, or gravitational segregation and may occur much more frequently than presently recognized (Betancourt *et al.*, 2009; Head *et al.*, 2003; Huang *et al.*, 2004; Khavari-Khorasani *et al.*, 1998; Larter *et al.*, 2006; Larter *et al.*, 2003; Mullins *et al.*, 2007a; Stainforth, 2004).

Figure 2 near here

Compositional gradients similar to those observed here often suggest reservoir compartmentalization. Compartmentalization can be assessed though pressure surveys and petrophysical logs, although those techniques suffer significant limitations (see Introduction). Figure 3 presents such measurements, showing constant pressure gradients and the absence of any obvious sealing barriers. This result suggests that the observed compositional grading exists in a single

connected reservoir, and the remainder of the manuscript demonstrates how such compositional grading can be used to assess reservoir connectivity with greater confidence than is available from pressure surveys and petrophysical logs alone.

Figure 3 near here

3. Experimental:

The composition of these three oil samples is investigated by use of comprehensive two-dimensional gas chromatography (GC×GC), electrospray ionization Fourier transform ion cyclotron resonance mass spectrometry (ESI FT-ICR MS), and optical spectroscopy.

3.1 GC×GC

GC×GC is a multidimensional version of gas chromatography (GC) in which components are separated according to two distinct chemical properties (Frysinger *et al.*, 2002). The second dimension of separation greatly enhances the resolution of the technique, and for complex mixtures such as crude oil and environmental samples the number of components resolved with GC×GC exceeds that resolved with traditional GC by an order of magnitude (Arey *et al.*, 2007; Arey *et al.*, 2005; Bertsch, 2000; Betancourt *et al.*, 2009; Gaines *et al.*, 2006; Liu and Lee, 2000; Phillips and Beens, 1999; Prazen *et al.*, 2001; Wang and Walters, 2007). The instrumentation used for this measurement has been described previously, and details particular to this application are presented as Supplementary Material (Betancourt *et al.*, 2009; Nelson *et al.*, 2006).

This implementation of GC×GC separates components of the non-polar fraction of petroleum according to their volatility and polarizability. GC×GC data are typically represented using a two-dimensional contour plot, with color representing magnitude and the values of the x and y axes representing the two retention times (Figure 4). Although this representation differs from traditional

GC-MS data, previous studies have demonstrated that direct comparisons between GC×GC and GC-MS show excellent abundance correlation and identities for petroleum biomarkers (Frysinger and Gaines, 2001). Moreover, in GC×GC the mass spectrum of each compound is not affected by other compounds that might co-elute in GC-MS, due to the increased resolving power and the absence of column bleed (Gaines *et al.*, 2006).

3.2 ESI FT-ICR MS

Electrospray ionization Fourier transform ion cyclotron resonance mass spectrometry is a high resolution mass spectrometric technique that permits determination of the elemental formulas of most components in a complex mixture (Marshall *et al.*, 1998). In the application described here, ESI FT-ICR MS is not used to detect the effluent of a GC; rather the crude oil is analyzed without prior separation. The benefit of this technique is that ESI FT-ICR MS is sensitive to the polar and high molecular weight fraction of crude oil, providing access to an important class of petroleum that is not detected by GC (Hughey *et al.*, 2002b). FT-ICR MS is considered the highest-resolution technique for investigating the composition of the asphaltene fraction, which is relevant to flow assurance, wettability, upgrading, and many other aspects of petroleum (Mullins *et al.*, 2007b).

Unlike the 70 eV electron ionization that is commonly employed in GC-MS analysis, electrospray ionization (ESI) is a soft ionization technique that ionizes polar components of petroleum without fragmentation or formation of multiply charged ions (Hughey *et al.*, 2002b; Zhan and Fenn, 2000); instead, singly charged molecular ions are detected. The soft ionization of petroleum molecules provided by ESI has been corroborated by good agreement of molecular weights measured by ESI with those measured by other soft ionization techniques such as two-step laser mass spectrometry (Hortal *et al.*, 2007; Hortal *et al.*, 2006; Pomerantz *et al.*, 2008; Pomerantz *et al.*, 2009; Rodgers and Marshall, 2007). ESI FT-ICR MS is useful for the analysis of complex mixtures because each elemental composition

($C_cH_hN_nO_oS_s$) has a unique molecular mass. With the high mass resolution and accuracy of ESI FT-ICR MS, more than 10,000 peaks in the mass spectrum of a crude oil can be resolved and their chemical formulae identified (Hughey *et al.*, 2002a; Hughey *et al.*, 2002b; Marshall and Rodgers, 2004; Marshall and Rodgers, 2008). Unlike GC, mass spectrometry of unfragmented ions does not in general distinguish isomers, although it is possible to distinguish 5- from 6- membered nitrogen heterocycles (Purcell *et al.*, 2007). However, ESI FT-ICR MS can provide a detailed chemical composition of the polar components of petroleum not detected by GC. Hence, ESI FT-ICR MS and GC×GC can be combined to provide a detailed description of the composition of almost an entire crude oil. The ESI FT-ICR MS method has been described previously, and details particular to this application are presented as Supplementary Material (Betancourt *et al.*, 2009; Mullins *et al.*, 2006; Senko *et al.*, 1996).

3.3 Optical spectroscopy

Optical spectra of crude oils are recorded by traditional techniques. The oils are diluted in CCl_4 to reduce scattering. Optical absorption in the range 500 – 800 nm is proportional to the relative asphaltene content of the oils (Mullins *et al.*, 2007a). Optical spectroscopy involves far less wet chemistry than traditional measures of determining asphaltene content such as SARA (saturates-aromatics-resins-asphaltenes) analysis and has been shown to provide more accurate measurements of relative asphaltene content in related oils than is typically achieved in SARA analysis. (Mullins *et al.*, 2007a) Based on optical absorption at different wavelengths in this range, the error associated with the spectroscopy is less than 1% of the average value. The actual error in the technique is likely larger because some wet chemistry is involved in preparing the sample for spectroscopic analysis. In this case the ratio of the asphaltene contents of the xx17 oil and the xx70 oil agree within 10% for optical spectroscopy and SARA analysis, although that result is potentially dominated by experimental error in the SARA technique.

4. Results

4.1 GC×GC

Figure 4 and table 1 near here

The oils studied here have high viscosities and asphaltene contents relative to most conventional crude oils (see Figure 2). High viscosity and asphaltene content in petroleum are usually associated with either low thermal maturity or post-generative degradational processes, most commonly biodegradation; therefore, biomarkers relating to thermal maturity and biodegradation are examined to understand the origin of this high viscosity and asphaltene content (Peters *et al.*, 2005; Zumberge, 1987). Figure 4 shows the GC×GC chromatogram for one of the oils. Chromatograms for the other two oils (not shown) are equivalent within typical experimental error; the full names of compounds identified in Figure 4 are presented in Table 1. Figure 5 and Table 2 present various maturity and source correlation parameters for the three oils extracted from the chromatograms. One set of biomarker ratios useful for assessing thermal maturity are the 22S/22(S+R) ratios for the C_{31} – C_{35} 17α-hopanes. The ratios for these oils (0.53 – 0.78) have reached their equilibrium values (0.55 – 0.62), suggesting that the main phase of oil generation has been reached or surpassed (Peters *et al.*, 2005). It is notable that this ratio increases for higher carbon number hopanes, as has been observed previously (Zumberge, 1987). The 22S/22(S+R) ratio potentially is influenced by biodegradation, with 22R being more susceptible. If biodegradation were affecting these hopanes, the 22S/22(S+R) would likely be greater than observed here and the ratio would decrease for larger carbon number hopanes, opposite of what is observed here. Hence the

22S/22(S+R) ratios for the C_{31} – C_{35} 17α-hopanes are likely robust maturity indicators for these oils. Another set of biomarker ratios useful for assessing thermal maturity are the 20S/20(S+R) ratios for the C27 ααα steranes. The ratios for these oils (0.44 – 0.49) are near their equilibrium values (0.52 – .055), consistently suggesting that these samples have reached the peak phase of oil generation (Peters *et al.*, 2005).

Figure 5 and Table 2 near here

As shown in the top panel of Figure 4, these oils contain essentially unaltered normal and isoprenoid alkanes, suggesting only light biodegradation. However, the highlighted section of Figure 4 (expanded in the bottom panel) demonstrates the presence of a sequence of 25-norhopanes. Although several theories explaining the interpretation of 25-norhopanes have been offered, it is commonly accepted that the presence of 25-norhopanes suggests extensive biodegradation; perhaps the most accepted theory suggests that a major mechanism in the appearance of 25-norhopanes is the biodegradation of hopanes, such that an oil containing an abundant sequence of 25-norhopanes must have experienced biodegradation to a level of at least 6 on the scale of Peters and Moldowan (PM 6) (Bennett *et al.*, 2006; Moldowan and McCaffrey, 1995; Peters and Moldowan, 1993; Peters *et al.*, 1996; Peters *et al.*, 2005; Seifert and Moldowan, 1979; Volkman *et al.*, 1983). It is possible for 25-norhopanes to occur in unaltered oils, but in those cases the concentration of 25-norhopanes is below the 3 ppm level detected here and a homologous series of 25-norhopanes is not observed (Moldowan and McCaffrey, 1995).

The simultaneous presence of unaltered alkanes and 25-norhopanes may appear to imply a contradiction: the unaltered alkanes indicate light biodegradation whereas the 25-norhopanes indicate severe biodegradation. However, this observation can be explained if the oil is considered to contain a mixture of lightly and heavily biodegraded oils (Nascimento *et al.*, 1999; Pan *et al.*, 2003; Philp, 1983; Rooney *et al.*, 1998; Volkman *et al.*, 1983). Thus, this assemblage of biomarkers is consistent with a reservoir mechanism involving at least two charges, with an earlier charge experiencing heavy biodegradation while a subsequent charge is essentially unaltered by microbes.

4.2 ESI FT-ICR MS

Detailed analysis of the nonpolar fraction of petroleum is attractive due to the relative experimental accessibility and the availability of a large body of literature relevant to its interpretation. However, the composition of the polar fraction of petroleum should not be neglected, especially when high asphaltene content oils are involved. A detailed measure of the composition of the polar fraction of these three oils can be obtained from ESI FT-ICR MS and some of the data are presented in Figure 6. This plot shows the relative abundance of different O_2 species (molecular formula: $C_cH_hO_2$) as a function of carbon number (c) and double bond equivalents (DBE); DBE is the number of rings plus double bonds to carbon in a compound and for O_2 species is computed as DBE = $c - h/2 + 1$. In addition, Figure 7 shows the DBE distribution for O_2 species obtained by summing the relative abundances over all carbon numbers; this plot contains less information than Figure 6 but is more readable.

Figures 6 and 7 near here

Kim et al. (2005) proposed a parameter that can assess the extent of biodegradation in oils from the same source rock based on data such as that shown in Figure 7. They find that O_2 species typically

correspond to naphthenic acids and that the ratio of acyclic O_2 species (DBE = 1.5 for the detected deprotonated species, corresponding to the carbonyl bond in the carboxylic acid group and no rings) to cyclic O_2 species (sum of species of DBE = 2.5, 3.5, and 4.5 for the detected deprotonated species) correlates well with the biodegradation (PM) scale of Peters and Moldowan (1993): the acyclic:cyclic ratio decreases with more extensive biodegradation due to the preferential mineralization of saturated naphthenic acids. The oils studied here are found to have acyclic:cyclic naphthenic acid ratios near 1:20, corresponding to a biodegradation index of approximately PM 4. The acyclic:cyclic naphthenic acid ratios of these three oils are constant within a factor of two, whereas acyclic:cyclic naphthenic acid ratios ranging over three orders of magnitude have been observed previously, again indicating the compositional similarity of these oils. A slightly higher abundance of cyclic naphthenic acids may exist in the xx70 oil relative to the xx17 and xx51 oils, but the well-known matrix effect in electrospray ionization makes such a small difference difficult to interpret without the use of naphthenic acid internal standards. given the well-known matrix effect in electrospray ionization.

There is currently no known way to identify a multiple charge history from the composition of an oil's polar fraction in analogy to the above-mentioned non-polar fraction analysis. However, a biodegradation index of PM 4 is consistent with the hypothesis that the oils studied result from commingling of a charge having biodegradation index of at least PM 6 with another charge having PM 0 or 1. Hence, ESI FT-ICR MS results are consistent with those from GC×GC, even though the two experiments examine different fractions of the oils, thereby increasing confidence in the analysis.

5. Origin of the compositional gradient

The GC×GC and ESI FT-ICR MS measurements suggest that these petroleum samples are mixtures of multiple charges including at least one charge that experienced extensive biodegradation.

The contribution of the biodegraded oil accounts for the high viscosity and asphaltene content. However, this analysis alone does not explain the steep gradients observed in Figure 2. The detailed composition of the fluids measured by GC×GC and ESI FT-ICR MS shows virtually no variation between the three samples, even though the viscosity varies by a factor of two. Although GC×GC and ESI FT-ICR MS provide excellent measures of the detailed composition of the nonpolar and polar ends of petroleum respectively, those techniques are less appropriate for measuring the abundance of broad chemical classes in the oil. Figure 8 presents the relative color of the oil samples, which is linearly proportional to their asphaltene content. Although the detailed composition of these samples varies little with depth, the asphaltene content (a much coarser measure of composition) is found to vary to a great extent. It is noteworthy that neither GC×GC nor ESI FT-ICR MS, the two best techniques for analyzing the detailed compositions of complex mixtures, readily detect a bulk quantity such as the variation in asphaltene content that is easily observed by the comparatively coarse optical spectroscopy. This result reinforces the notion that multiple techniques—detailed and bulk—are presently required for accurate characterization of the composition of petroleum.

Figure 8 near here

A similar increase in the relative asphaltene content with depth has been observed in other reservoirs and has been modeled as a Boltzmann distribution with the Archimedes buoyancy in the energy term (Betancourt *et al.*, 2009; Mullins *et al.*, 2007a). This model assumes that the only cause of grading in asphaltene content is gravitational segregation (Khavari-Khorasani *et al.*, 1998) of dense asphaltene nanoaggregates toward the bottom of the reservoir at equilibrium, and the only adjustable parameter in the model is the size of the asphaltene nanoaggregate. This equilibrium model assumes

that although the concentration of heavy ends varies in the reservoir, their composition is mostly unchanged; that assumption is supported in this case by the similarity of the ESI FT-ICR MS data for the three samples (Figure 6). Figure 8 includes a fit of the measured relative asphaltene content versus depth to the Boltzmann-Archimedes model. The fitted nanoaggregate size is 2.0 nm, which is consistent with asphaltene nanoaggregate sizes measured in other crude oil reservoirs (Betancourt *et al.*, 2009; Mullins *et al.*, 2007a) as well as measured in solvents by various laboratory techniques: ultrasonics (Andreatta *et al.*, 2005), magnetic resonance (Kawashima *et al.*, 2008; Lisitza *et al.*, 2009), electrical conductivity (Zeng *et al.*, 2009), and centrifugation (Mostowfi *et al.*, 2009). This agreement suggests that the observed grading in asphaltene content can be explained solely by gravitational segregation of dense asphaltene nanoaggregates.

Lin et al. (1995) demonstrated that the viscosity of an asphaltene containing mixture increases faster than exponentially with asphaltene content. Hence, for oils containing more than a few percent asphaltenes, the viscosity should increase dramatically for a small increase in asphaltene content. Indeed, the observed doubling in viscosity is consistent with Lin and coworkers' measurements for ~20% variation in the asphaltene content of oils having ~ 10 wt% asphaltenes, as is the case here. Therefore, the origin of the viscosity gradient can be explained: the viscosity gradient results from a gradient in asphaltene content due to gravitational segregation in a series of oils that contain high asphaltene content as a result of extensive biodegradation in at least one of the multiple charges that filled the reservoir.

6. Assessment of Reservoir Connectivity

Reservoir connectivity is among the most important uncertainties for petroleum production and geochemical studies. Thus, any technique to address connectivity that can be performed prior to the

expensive operation of producing reservoir fluids has value. Connectivity is presently assessed though pressure surveys, petrophysical logs, and geochemical fingerprints, but each of those techniques can fail to recognize compartmentalization (Mullins, 2008). Here we present a novel technique for assessing connectivity. This analysis is based on different physics than the conventional methods, and a combination of this analysis with conventional analyses can assess connectivity with greater confidence than is achievable with conventional analyses alone.

In this reservoir, these three traditional techniques all suggest good connectivity. In particular, a pressure survey shows a constant gradient and the gamma-ray log shows no indication of a sealing barrier. The GC×GC and ESI FT-ICR MS measurements provide exquisitely detailed fingerprints of almost the entire petroleum, and in this reservoir those fingerprints are nearly identical, positively constraining connectivity almost as tightly as possible with fingerprinting techniques.

Simultaneously, compositional grading is observed in this reservoir, with pronounced gradients in the fluids' viscosity, asphaltene content, and density over a 53 m interval. Such compositional grading is often associated with reservoir compartmentalization. However, there are several notable examples of extensive compositional grading in connected reservoirs (Betancourt *et al.*, 2009; Mullins *et al.*, 2007a); Figure 9 presents an extreme example from a field in which a single oil column contains oils with obvious compositional variations. In fact, connected reservoirs at or near equilibrium must exhibit compositional grading due to gravitational segregation and potentially other forces (Khavari-Khorasani *et al.*, 1998; Larter *et al.*, 2006). The observation of such compositional grading with the correct magnitude provides another indication of connectivity based on different reservoir physics than the three standard measurements. For the present work, in addition to the traditional techniques and a gradient in asphaltene content, connectivity is suggested by gradients in fluid density and viscosity. The consistency of the magnitude of the viscosity gradient with predictions from the magnitude of the

asphaltene content gradient further supports connectivity. Moreover, a reservoir history involving multiple charging events was established which suggests that asphaltenes have achieved an equilibrium distribution but were initially out of equilibrium (Khavari-Khorasani *et al.*, 1998; Larter *et al.*, 2006; Larter *et al.*, 2003); this migration on the reservoir scale of the least mobile fraction strongly suggests good vertical connectivity. Therefore, addition of biomarker analysis and observation of bulk compositional gradients of the proper magnitude positively constrain connectivity more tightly than is possible with only the conventional techniques of pressure surveys, petrophysical logs, and geochemical fingerprints.

7. Conclusion

Three oil samples collected from well-defined depths spanning a 53 m interval in the same well exhibit marked gradients in viscosity, asphaltene content, and API gravity while pressure surveys, petrophysical logs, and geochemical fingerprints suggest that the oils come from a single, connected reservoir. The compositions of these fluids are studied with detailed and bulk measurements to determine the origin of the compositional grading: GC×GC probes the detailed composition of the non-polar fraction, negative ion ESI FT-ICR MS probes the detailed composition of the polar fraction, and optical spectroscopy measures the bulk distribution of light and heavy ends. The combination of GC×GC and ESI-FT-ICR MS provides a detailed measurement of the composition of almost the entire petroleum, but optical spectroscopy provides important information about bulk composition absent from the detailed measurements alone.

GC×GC experiments detect the simultaneous presence of unaltered normal and isoprenoid alkanes as well as 25-norhopanes, which is interpreted to indicate a mixture of multiple charges with one charge having been extensively biodegraded. ESI FT-ICR MS experiments are sensitive to a separate

fraction of petroleum but provide consistent results. Hence, the high asphaltene content in these oils (10% by weight) originates from early biodegradation of the initial charge. Additionally, the asphaltene content of these oils increases with depth, which can be explained by a Boltzmann-Archimedes model that considers only gravitational segregation of dense asphaltene nanoaggregates. Increases in asphaltene content are known to increase the viscosity of oils, and the magnitude of the viscosity increase observed here is consistent with the asphaltene gradient. Therefore, the viscosity gradient arises from gravitational segregation of asphaltenes in a fluid with high asphaltene content due to a highly biodegraded charge.

The compositional grading described here results from gravitational segregation and hence must exist in every connected reservoir at or near equilibrium. Therefore, the identification of such gradients of the correct magnitude represents another test of reservoir connectivity based on different physics from the traditional techniques of pressure surveys, petrophysical logs, and geochemical fingerprints. Combining this analysis of continuous gradients of predictable magnitudes with traditional measurements constrains reservoir connectivity much more tightly than is possible with current techniques prior to the expensive process of producing the reservoir. In this example, a biomarker study establishes a reservoir history involving reservoir-scale migration of relatively immobile asphaltenes, and this reservoir history positively constrains connectivity even further.

7. Acknowledgements

The authors acknowledge the reviewers for their helpful comments. The mass spectrometry work was supported by the NSF Division of Materials Research through DMR-06-54118, and the State of Florida.

Table 1:

Compound ID	Compound Name	Molecular Weight (g/mol)
	Hopanes, Moretanes, and Gammacerane	
Ts	18α(H)-22,29,30-trinorneohopane (C27H46)	370
Tm	17α(H)-22,29,30-trinorhopane (C27H46)	370
BNH	17α(H),21β(H)-28,30-bisnorhopane (C28H48)	384
NH	17α(H),21β(H)-30-norhopane (C29H50)	398
NM	17β(H),21α(H)-30-norhopane (C29H50)	398
H	17α(H),21β(H)-hopane (C30H52)	412
M	17β(H),21α(H)-hopane (C30H52)	412
HH (S)	17α(H),21β(H)-22S-homohopane (C31H54)	426
HH (R)	17α(H),21β(H)-22R-homohopane (C31H54)	426
G	Gammacerane	412
2HH (S)	17α(H),21β(H)-22S-bishomohopane (C32H56)	440
2HH (R)	17α(H),21β(H)-22R-bishomohopane (C32H56)	440
3HH (S)	17α(H),21β(H)-22S-trishomohopane (C33H58)	454
3HH (R)	17α(H),21β(H)-22R-trishomohopane (C33H58)	454
4HH (S)	17α(H),21β(H)-22S-tetrakishomohopane (C34H60)	468
4HH (R)	17α(H),21β(H)-22R-tetrakishomohopane (C34H60)	468
5HH (S)	17α(H),21β(H)-22S-pentakishomohopane (C35H62)	482
5HH (R)	17α(H),21β(H)-22R-pentakishomohopane (C35H62)	482
	25-Norhopanes	
25-nor-Tm	17α(H)-22,25,29,30-tetranorhopane (C26H44)	356
25-nor-BNH	17α(H),21β(H)-25,28,30-trinorhopane (C27H46)	370
25-nor-NH	17α(H),21β(H)-25,30-bisnorhopane (C28H48)	384
25-nor-H	17α(H),21β(H)-25-norhopane (C29H50)	398
25-nor-HH (S)	17α(H),21β(H)-22S-25-norhomohopane (C30H52)	412
25-nor-HH (R)	17α(H),21β(H)-22R-25-norhomohopane (C30H52)	412
25-nor-2HH (S)	17α(H),21β(H)-22S-25-norbishomohopane (C31H54)	426
25-nor-2HH (R)	17α(H),21β(H)-22R-25-norbishomohopane (C31H54)	426
25-nor-3HH (S)	17α(H),21β(H)-22S-25-nortrishomohopane (C32H56)	440

Table caption: Full names of compounds identified in the lower panel of Figure 4.

Table 2:

Depth (m)	Pr/ Ph[1]	Pr/ *n*-C_{17}[2]	Ph/ *n*-C_{18}[3]	C_{27} DiaSt S/ (S+R)[4]	C_{30} TT S/(S+R)[5]	C_{23} TT/ Hop[6]	Ts/ (Ts+Tm)[7]	C_{27} Hop/ C_{29} Hop[8]	C_{29}Hop/ C_{30} Hop[8]	C_{30} Hop/ C_{31} Hop[8]
xx17	1.39	0.94	0.97	0.58	0.38	0.21	0.29	0.38	0.77	1.39
xx51	1.39	0.93	0.98	0.55	0.37	0.22	0.28	0.38	0.80	1.36
xx70	1.39	0.94	0.99	0.59	0.40	0.21	0.28	0.38	0.76	1.41

Depth (m)	Mor/ Hop[9]	C_{31} Hop S/(S+R)[10]	C_{32} Hop S/(S+R)[10]	C_{33} Hop S/(S+R)[10]	C_{34} Hop S/(S+R)[10]	C_{35} Hop S/(S+R)[10]
xx17	0.15	0.58	0.53	0.66	0.71	0.73
xx51	0.16	0.60	0.57	0.66	0.76	0.73
xx70	0.15	0.58	0.57	0.66	0.78	0.69

Table Caption: Source correlation and thermal maturity parameters for the three oil samples. Biomarker ratios are calculated from integrated GC×GC-FID peak volumes. Full names of compounds are listed below.

[1] Pr/Ph = pristane/phytane.

[2] Pr/*n*-C_{17} = pristane/heptadecane.

[3] Ph/*n*-C_{18} = phytane/octadecane.

[4] C_{27} DiaSt S/(S+R) = C_{27} diacholestane 20S/20(S+R).

[5] C_{30} TT S/(S+R) = C_{30} tricyclic terpane 22S/22(S+R).

[6] C_{23} TT/Hop = C_{23} tricyclic terpane/(C_{23} tricyclic terpane + C_{30} 17α(H),21β(H)-hopane).

[7] Ts/(Ts+Tm) = C_{27} 17α(H)-22,29,30-trisnorhopane and 18α(H)-22,29,30-trisnorhopane, respectively.

[8] C_{27} Hop/C_{29} Hop = (Ts +Tm)/C_{29} 17α(H),21β(H)-hopane; C_{29} Hop/C_{30} Hop = C_{29} 17α(H),21β(H)-hopane/C_{30} 17α(H),21β(H)-hopane; C_{30} Hop/C_{31} Hop = C_{30} 17α(H),21β(H)-hopane/C_{31} 17α(H),21β(H)-hopane 22(S +R).

[9] Mor/Hop = mortane/hopane.

[10] C_{31}S/(S+R) = C_{31} 17α(H),21β(H)-homohopane 22S/C_{31} 17α(H),21β(H)-homohopane 22(S+R) higher carbon number series follow the same formula.

Figure Captions:

Figure 1) Schematic diagram of the sampling tool that acquires crude oil samples and performs optical spectral analysis on these samples for a chemical analysis in situ in the oil well. This tool is used in open-hole just after the well is drilled and prior to casing the well. The probe (pictured) is pressed firmly against the borehole wall to make hydraulic communication with permeable zones in the oil well to extract formation fluids.

Figure 2) Viscosity (dead oil at room temperature), asphaltene content, and API gravity of the three samples, plotted as a function of depth. Viscosity is reported in centipoise (cP).

Figure 3) Wireline well log. The first track shows the gamma-ray log; no obvious vertical lithological barriers are indicated in the reservoir section. The first track also shows a continuous pressure profile.

Figure 4) GC×GC chromatogram for the xx17 m oil. The top panel shows the total ion count for the entire two-dimensional chromatographic plane. The bottom panel focuses on the region containing the 25-norhopane peaks and shows the summed counts for the ions of m/z = 177 and 191; this region is indicated in the yellow dotted box in the top panel. The simultaneous presence of unaltered normal and isoprenoid alkanes (top panel) and 25-norhopanes (bottom panel) implies that the measured oil is a mixture of at least one lightly biodegraded charge with at least one heavily biodegraded charge.

Figure 5) Spider plot of several oil source correlation and thermal maturity parameters. The compositions of the three different oils are barely discernible: xx17 m in blue, xx51 m in red, and xx70 m in green. Full names of these molecules are provided in Table 1. These ratios, especially the 22S/22(S+R) ratios for the C_{31} – C_{35} 17α-hopanes, suggest that the main phase of oil generation has been reached or surpassed.

Figure 6) Isoabundance-contours for plots of double bond equivalents (DBE) vs. carbon number for O_2 species from each of the three oils.

Figure 7) Double bond equivalents (DBE) distribution for the O_2 class of each oil. From this display the acyclic:cyclic ratio of naphthenic acids is determined and found to correlate with a biodegradation rank of PM 4.

Figure 8) Markers: relative asphaltene content of the three oils, determined by optical spectroscopy, plotted as a function of depth. Line: fit to the Boltzmann-Archimedes model. This fit results in an asphaltene nanoaggregate size of 2.0 nm, consistent with other reservoirs and laboratory studies and suggesting that the gradient in asphaltene content can be explained solely by gravitational segregation.

Figure 9) Compositional grading in a series of dead oils from different depths in a single oil column. Oils are aligned from the shallowest at left to the deepest at right. Ccourtesy of Hani Elshahawi, Shell International E&P.

Figure 1)

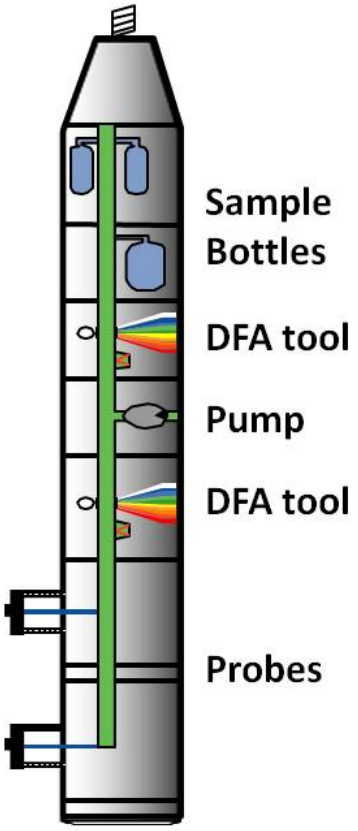

Probe (extended)

Figure 2)

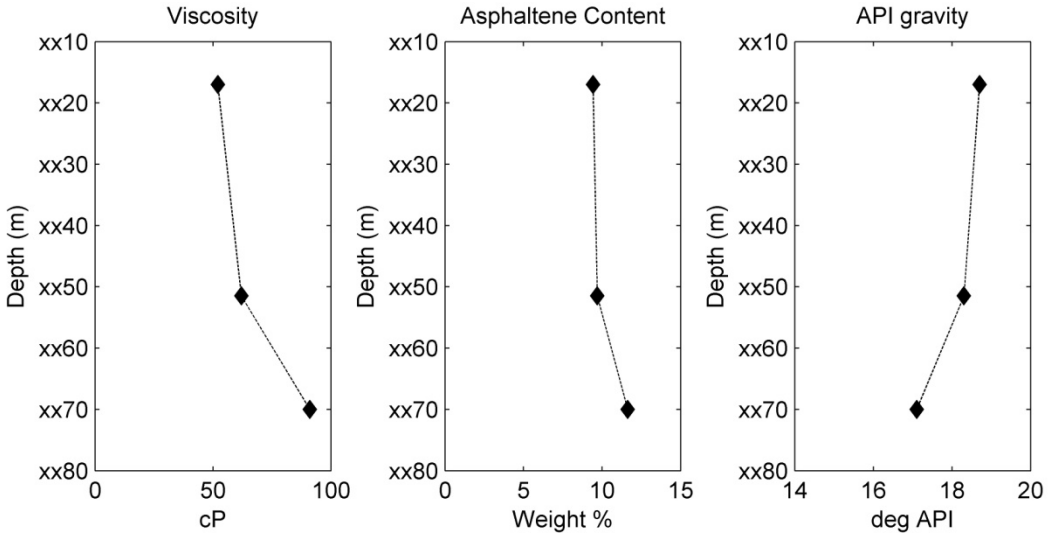
Viscosity
Asphaltene Content
API gravity
Depth (m)
xx10
xx20
xx30
xx40
xx50
xx60
xx70
xx80
0
50
100
cP
0
5
10
15
Weight %
14
16
18
20
deg API

Figure 3)

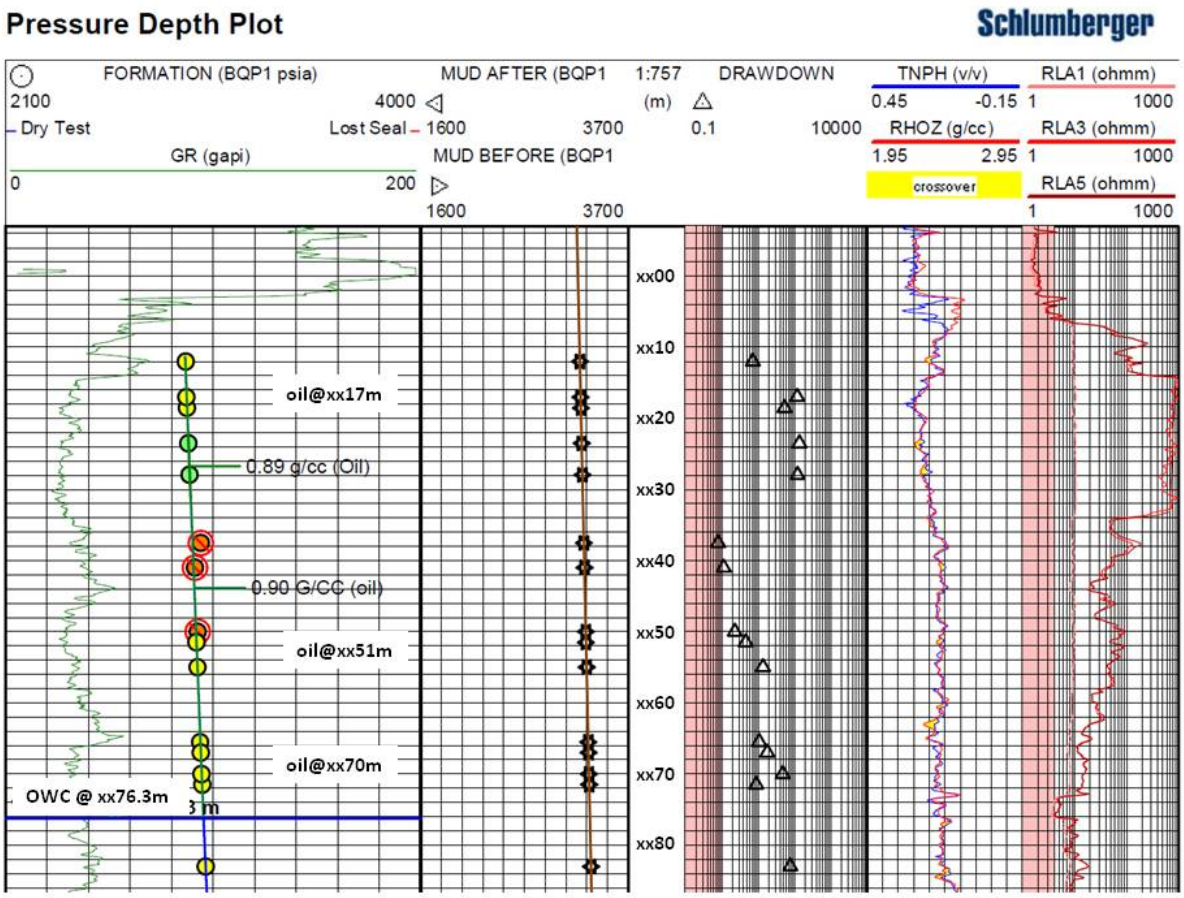
Pressure Depth Plot
Schlumberger
FORMATION (BQP1 psia)
2100
4000
Dry Test
Lost Seal
GR (gapi)
0
200
MUD AFTER (BQP1
1600
3700
MUD BEFORE (BQP1
1600
3700
1:757
(m)
DRAWDOWN
0.1
10000
TNPH (v/v)
0.45
-0.15
RHOZ (g/cc)
1.95
2.95
crossover
RLA1 (ohmm)
1
1000
RLA3 (ohmm)
1
1000
RLA5 (ohmm)
1
1000
xx00
xx10
xx20
xx30
xx40
xx50
xx60
xx70
xx80
oil@xx17m
0.89 g/cc (Oil)
0.90 G/CC (oil)
oil@xx51m
oil@xx70m
OWC @ xx76.3m
3 m

Figure 4)

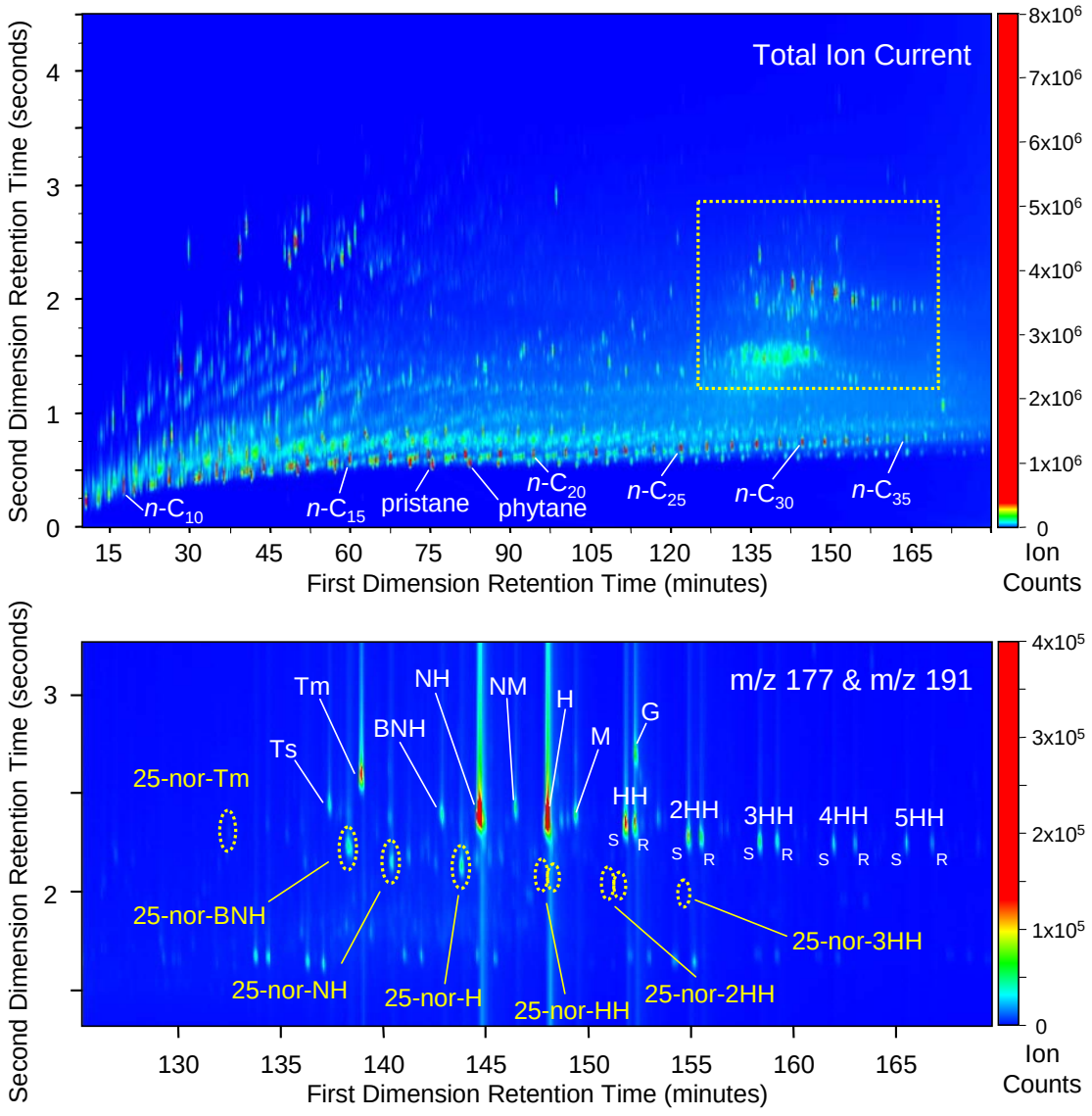
Total Ion Current
Second Dimension Retention Time (seconds)
First Dimension Retention Time (minutes)
Ion Counts
8x10^6
7x10^6
6x10^6
5x10^6
4x10^6
3x10^6
2x10^6
1x10^6
0
n-C10
n-C15
pristane
phytane
n-C20
n-C25
n-C30
n-C35
m/z 177 & m/z 191
4x10^5
3x10^5
2x10^5
1x10^5
Tm
NH
NM
H
G
M
BNH
Ts
25-nor-Tm
HH
2HH
3HH
4HH
5HH
S
R
25-nor-BNH
25-nor-3HH
25-nor-NH
25-nor-H
25-nor-HH
25-nor-2HH

Figure 5)

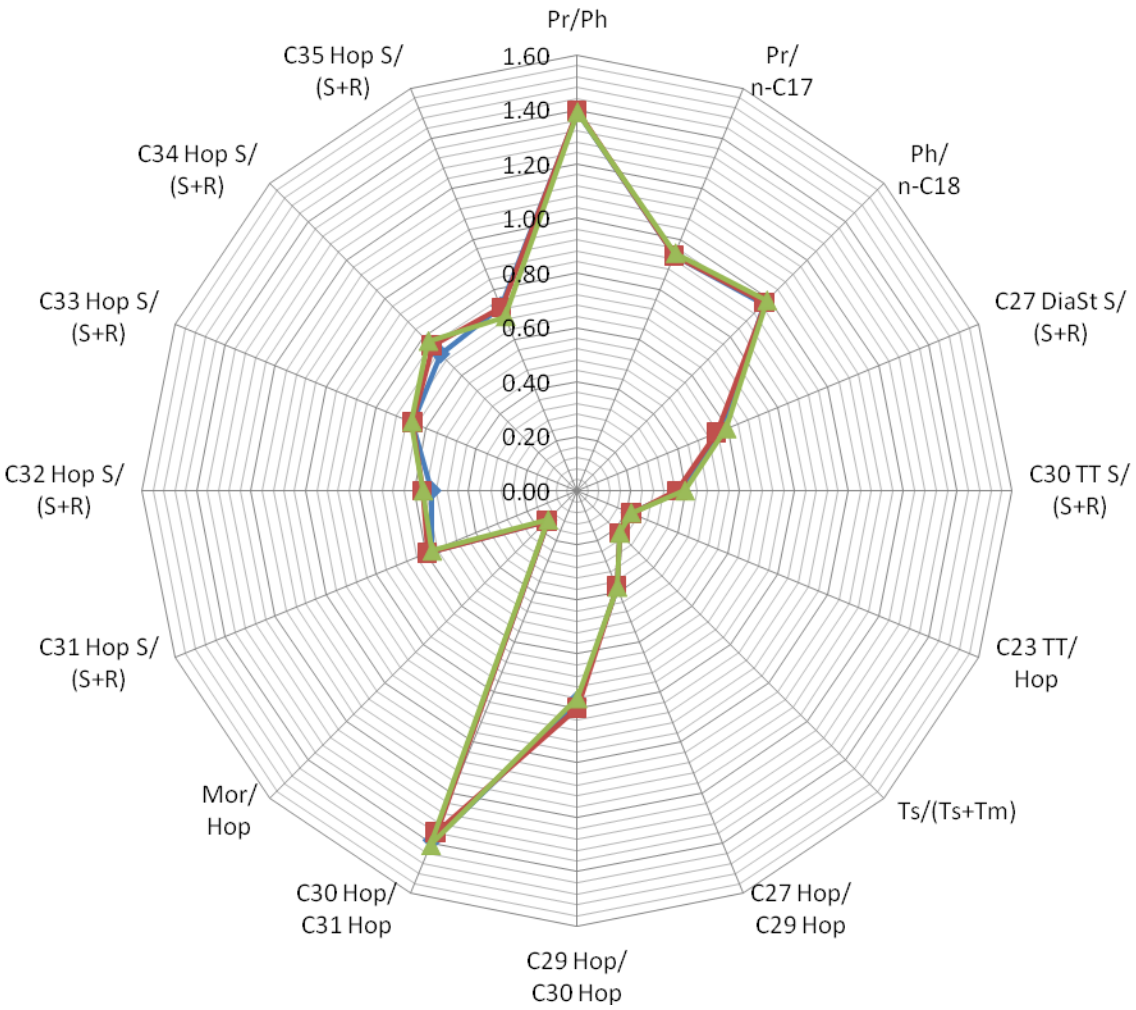
Pr/Ph
Pr/
n-C17
Ph/
n-C18
C27 DiaSt S/
(S+R)
C30 TT S/
(S+R)
C23 TT/
Hop
Ts/(Ts+Tm)
C27 Hop/
C29 Hop
C29 Hop/
C30 Hop
C30 Hop/
C31 Hop
Mor/
Hop
C31 Hop S/
(S+R)
C32 Hop S/
(S+R)
C33 Hop S/
(S+R)
C34 Hop S/
(S+R)
C35 Hop S/
(S+R)
1.60
1.40
1.20
1.00
0.80
0.60
0.40
0.20
0.00

Figure 6)

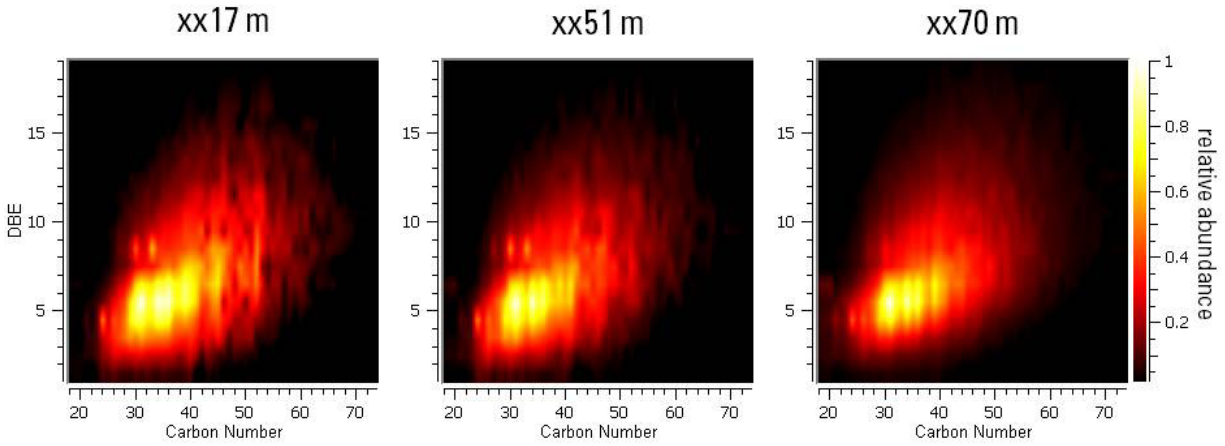

Figure 7)

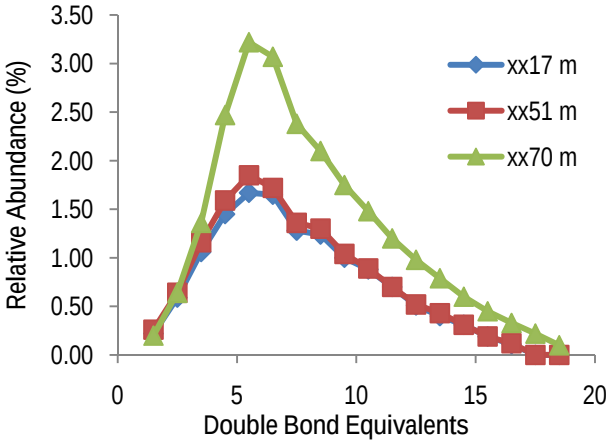
3.50
3.00
2.50
2.00
1.50
1.00
0.50
0.00
Relative Abundance (%)
0
5
10
15
20
Double Bond Equivalents
xx17 m
xx51 m
xx70 m

Figure 8)

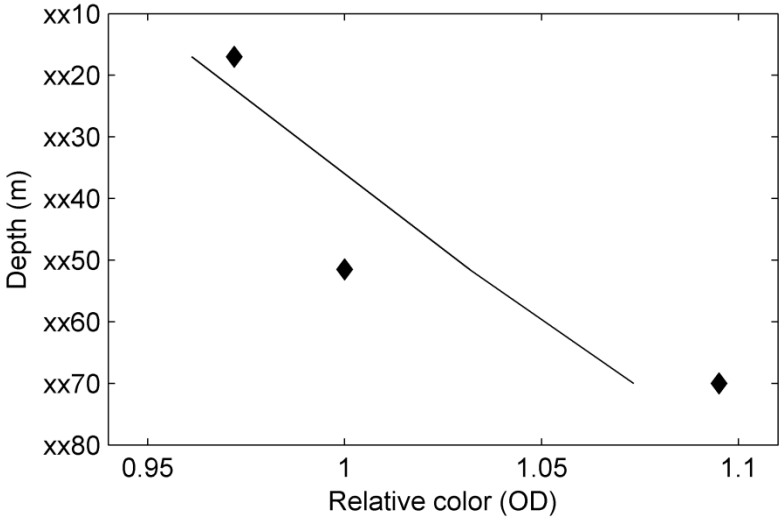
xx10
xx20
xx30
xx40
xx50
xx60
xx70
xx80
Depth (m)
0.95
1
1.05
1.1
Relative color (OD)

Figure 9)

References

Andreatta, G., Bostrom, N., Mullins, O.C., 2005. High-Q ultrasonic determination of the critical nanoaggregate concentration of asphaltenes and the critical micelle concentration of standard surfactants. Langmuir 21, 2728-2736.

Arey, J.S., Nelson, R.K., Reddy, C.M., 2007. Disentangling oil weathering using GC×GC. 1. Chromatogram analysis. Environmental Science and Technology 41, 5738-5746.

Arey, J.S., Nelson, R.K., Xu, L., Reddy, C.M., 2005. Using comprehensive two-dimesional gas chromatography retention indices to estimate environmental partitioning properties for a complete set of diesel fuel hydrocarbons. Analytical Chemistry 77, 7172-7182.

Bennett, B., Fustic, M., Farrimond, P., Huang, H., Larter, S.R., 2006. 25-norhopanes: Formation during biodegradation of petroleum in the subsurface. Organic Geochemistry 37, 787-797.

Bertsch, W., 2000. Two-dimensional gas chromatography. Concepts, instrumentation, and applications - part 2: Comprehensive two-dimensional gas chromatography. Journal of High Resolution Chromatography 23, 167-181.

Betancourt, S.S., Ventura, G.T., Pomerantz, A.E., Viloria, O., Dubost, F.X., Zuo, J., Monson, G., Bustamante, D., Purcell, J.M., Nelson, R.K., Rodgers, R.P., Reddy, C.M., Marshall, A.G., Mullins, O.C., 2009. Nanoaggregates of asphaltenes in a reservoir crude oil and reservoir connectivity. Energy and Fuels 23, 1178-1188.

Frysinger, G.S., Gaines, R.B., 2001. Separation and identification of petroleum biomarkers by comprehensive two-dimensional gas chromatography. Journal of Separation Science 24, 87-96.

Frysinger, G.S., Gaines, R.B., Reddy, C.M., 2002. GC x GC--a new analytical tool for environmental forensics. Environmental Forensics 3, 27-34.

Gaines, R.B., Frysinger, G.S., Reddy, C.M., Nelson, R.K.2006. Oil spill source identification by comprehensive two-dimensional gas chromatography (GC×GC). In: Z. Wang, S. Stout (Eds.), Oil spill fingerprinting and source identification. (Ed. by Z. Wang, S. Stout) Elsevier, pp. 169-206.

Head, I.M., Jones, D.M., Larter, S.R., 2003. Biological activity in the deep subsurface and the origin of heavy oil. Nature 426, 344-352.

Hetherington, G., Horan, A.J., 1960. Variations with elevation of Kuwait reservoir fluids. Journal of the Institute of Petroleum 46, 109-114.

Høier, L., Whitson, C.H., 2001. Compositional grading--theory and practice. SPE Reservoir Evaluation & Engineering SPE 74714, 525-535.

Hortal, A.R., Hurtado, P., Martínez-Haya, B., Mullins, O.C., 2007. Molecular weight distributions of coal and petroleum asphaltenes from laser desorption/ionization experiments. Energy and Fuels 21, 2863-2868.

Hortal, A.R., Martínez-Haya, B., Lobato, M.D., Pedrosa, J.M., Lago, S., 2006. On the determination of molecular weight distributions of asphaltenes and the aggregates in laser desorption ionization experiments. Journal of Mass Spectrometry 41, 960-968.

Huang, H., Bowler, B.F.J., Oldenburg, T.B.P., Larter, S.R., 2004. The effect of biodegradation on polycyclic aromatic hydrocarbons in reservoired oils from the Liaohe Basin, NE China. Organic Geochemistry 35, 1619-1634.

Hughey, C.A., Rodgers, R.P., Marshall, A.G., 2002a. Resolution of 11 000 compositionally distinct components in a single electrospray ionization Fourier transform ion cyclotron resonance mass spectrum of crude oil. Analytical Chemistry 74, 4145-4149.

Hughey, C.A., Rodgers, R.P., Marshall, A.G., Qian, K., Robbins, W.K., 2002b. Identification of acidic NSO compounds in crude oils of different geochemical origins by negative ion electrospray Fourier transform ion cyclotron resonance mass spectrometry. Organic Geochemistry 33, 743-759.

Kawashima, H., Takanohashi, T., Iino, M., Matsukawa, S., 2008. Determining asphaltene aggregation in solution from diffusion coefficients as determined by pulsed-field gradient spin-echo ^{1}H NMR. Energy and Fuels 22, 3989-3993.

Khavari-Khorasani, G., Michelsen, J.K., Dolson, J.C., 1998. The factors controlling the abundance and migration of heavy vs. light oils, as constrained by data from the Gulf of Suez. Part II. The significance of reservoir mass transport processes. Organic Geochemistry 29, 283-300.

Kim, S., Stanford, L.A., Rodgers, R.P., Marshall, A.G., Walters, C.C., Qian, K., Wenger, L.M., Mankiewicz, P., 2005. Microbial alteraction of the acidic and neutral polar NSO compounds revealed by Fourier transform ion cyclotron resonance mass spectrometry. Organic Geochemistry 36, 1117-1134.

Larter, S.R., Huang, H., Adams, J., Bennett, B., Jokanola, O., Oldenburg, T.B.P., Jones, D.M., Head, I.M., Riediger, C., Fowler, M., 2006. The controls on the composition of biodegraded oils in the deep subsurface: Part II--geological controls on subsurface biodegradation fluxes and constraints on reservoir-fluid property prediction. American Association of Petroleum Geologists Bulletin 90, 921-938.

Larter, S.R., Wilhelms, A., Head, I.M., Koopmans, M., Aplin, A., Di Primo, R., Zwach, C., Erdmann, M., Telnaes, N., 2003. The controls on the composition of biodegraded oils in the deep subsurface--part 1: Biodegradation rates in petroleum reservoirs. Organic Geochemistry 34, 601-613.

Lin, M.S., Lunsford, K.M., Glover, C.J., Davidson, R.R., Bullin, J.A.1995. The effects of asphaltenes on the chemical and physical characteristics of asphalt. In: E.Y. Sheu, O.C. Mullins (Eds.), Asphaltenes: Fundamentals and applications. (Ed. by E.Y. Sheu, O.C. Mullins) Plenum Press, New York, pp. 155-176.

Lisitza, N.V., Freed, D.E., Sen, P.N., Song, Y.-Q., 2009. Study of asphaltene nanoaggregation by nuclear magnetic resonance (NMR). Energy and Fuels 23, 1189-1193.

Liu, Z., Lee, M.L., 2000. Comprehensive two-dimensional separations using microcolumns. Journal of Microcolumn Separations 12, 241-254.

Marshall, A.G., Hendrickson, C.L., Jackson, G.S., 1998. Fourier transform ion cyclotron resonance mass spectrometry: A primer. Mass Spectrometry Reviews 17, 1-35.

Marshall, A.G., Rodgers, R.P., 2004. Petroleomics: The next grand challenge for chemical analysis. Accounts of Chemical Research 37, 53-59.

Marshall, A.G., Rodgers, R.P., 2008. Petroleomics: Chemistry of the underworld. Proceedings of the National Academy of Sciences of the United States of America 105, 18090-18095.

Moldowan, J.M., McCaffrey, M.A., 1995. A novel microbial hydrocarbon degradation pathway revealed by hopane demethylation in a petroleum reservoir. Geochimica et Cosmochimica Act 59, 1891-1894.

Mostowfi, F., Indo, K., Mullins, O.C., McFarlane, R., 2009. Asphaltene nanoaggregates studied by centrifugation. Energy and Fuels 23, 1194-1200.

Mullins, O.C., 2008. The physics of reservoir fluids: Discovery through downhole fluid analysis. Schlumberger, Sugar Land, TX.

Mullins, O.C., Betancourt, S.S., Cribbs, M.E., Dubost, F.X., Creek, J.L., Andrews, A.B., Venkataramanan, L., 2007a. The collodial structure of crude oil and the structure of oil reservoirs. Energy and Fuels 21, 2785-2794.

Mullins, O.C., Rodgers, R.P., Weinheber, P., Klein, G.C., Venkataramanan, L., Andrews, A.B., Marshall, A.G., 2006. Oil reservoir characterization via crude oil analysis by downhole fluid analysis in oil wells with visible--near-infrared spectroscopy and by laboratory analysis with electrospray

ionization Fourier transform ion cyclotron resonance mass spectrometry. Energy and Fuels 20, 2448-2456.
Mullins, O.C., Sheu, E.Y., Hammami, A., Marshall, A.G., 2007b. Asphaltenes, heavy oils, and petroleomics. Springer, New York.
Nascimento, L.R., Rebouças, L.M.C., Koike, L., Reis, F.d.A.M., Soldan, A.L., Cerqueira, J.R., Marsaioli, A.J., 1999. Acidic biomarkers from albacora oils, Campos Basin, Brazil. Organic Geochemistry 30, 1175-1191.
Nelson, R.K., Kile, B.M., Plata, D.L., Sylva, S.P., Xu, L., Reddy, C.M., Gaines, R.B., Frysinger, G.S., Reichenbach, S.E., 2006. Tracking the weathering on a oil spill with comprehensive two-dimensional gas chromatography. Environmental Forensics 7, 33-44.
Pan, C., Yang, J., Fu, J., Sheng, G., 2003. Molecular correlation of free oil and inclusion oil of reservoir rocks in the Junggar Basin, China. Organic Geochemistry 34, 357-374.
Peters, K.E., Moldowan, J.M., 1993. The biomarker guide: Interpreting molecular fossils in petroleum and ancient sediments. Prentine Hall, Englewood Cliffs, NJ.
Peters, K.E., Moldowan, J.M., McCaffrey, M.A., Fago, F.J., 1996. Selective biodegradation of extended hopanes to 25-norhopanes in petroleum reservoirs. Insights from molecular mechanics. Organic Geochemistry 24, 765-783.
Peters, K.E., Walters, C.C., Moldowan, J.M., 2005. The biomarker guide. Cambridge University Press, Cambridge.
Phillips, J.B., Beens, J., 1999. Comprehensive two-dimensional gas chromatography: A hyphenated method with strong coupling between the two dimensions. Journal of Chromatography A 856, 331-347.
Philp, R.P., 1983. Correlation of crude oils from the San Jorges Basin, Argentina. Geochimica et Cosmochimica Act 47, 267-275.
Pomerantz, A.E., Hammond, M.R., Morrow, A.L., Mullins, O.C., Zare, R.N., 2008. Two-step laser mass spectrometry of asphaltenes. Journal of the American Chemical Society 130, 7216-7217.
Pomerantz, A.E., Hammond, M.R., Morrow, A.L., Mullins, O.C., Zare, R.N., 2009. Asphaltene molecular-mass distribution determined by two-step laser mass spectrometry. Energy and Fuels 23, 1162-1168.
Prazen, B.J., Johnson, K.J., Weber, A., Synovec, R.E., 2001. Two-dimensional gas chromatography and trilinear partial least squares for the quantitative analysis of aromatic and naphthene content in naphtha. Analytical Chemistry 73, 5677-5682.
Purcell, J.M., Rodgers, R.P., Hendrickson, C.L., Marshall, A.G., 2007. Speciation of nitrogen containing aromatics by atmospheric pressure photoionization or electrospray ionization Fourier transform ion cyclotron resonance mass spectrometry. Journal of the American Society for Mass Spectrometry 18, 1265-1273.
Ratulowski, J., Fuex, A.N., Westrich, J.T., Sieler, J.J., 2003. Theoretical and experimental investigation of isothermal compositional grading. SPE Reservoir Evaluation & Engineering SPE 84777, 168-175.
Rodgers, R.P., Marshall, A.G.2007. Petroleomics: Advanced characterization of petroleum-derived materials by fourier transform ion cyclotron resonance mass spectrometry (FT-ICR MS). In: O.C. Mullins, E.Y. Sheu, A. Hammami, A.G. Marshall (Eds.), Asphaltenes, heavy oils, and petroleomics. (Ed. by O.C. Mullins, E.Y. Sheu, A. Hammami, A.G. Marshall) Springer, New York, pp. 63-93.
Rooney, M.A., Vuletich, A.K., Griffith, C.E., 1998. Compound-specific isotope analysis as a tool for characterizing mixed oils: An examples form the West of Shetlands area. Organic Geochemistry 29, 241-254.
Seifert, W.K., Moldowan, J.M., 1979. The effect of biodegradation on steranes and terpanes in crude oil. Geochimica et Cosmochimica Act 43, 111-126.

Senko, M.W., Hendrickson, C.L., Paša-Tolić, L., Marto, J.A., White, F.M., Guan, S., Marshall, A.G., 1996. Electrospray ionization Tourier transform ion cyclotron resonance at 9.4 T. Rapid Communications in Mass Spectrometry 10, 1824-1828.

Stainforth, J.G.2004. New insights into reservoir filling and mixing processes. In: J.M. Cubitt, W.A. England, S.R. Larter (Eds.), Understanding petroleum reservois: Towards an integrated reservoir engineering and geochemical approach. 237. (Ed. by J.M. Cubitt, W.A. England, S.R. Larter) Geological Society, London, pp. 115-132.

Volkman, J.K., Alexander, R., Kagi, R.I., Woodhouse, G.W., 1983. Demthylated hopanes in crude oil and their applications in petroleum geochemistry. Geochimica et Cosmochimica Act 47, 785-794.

Wang, F.C.-Y., Walters, C.C., 2007. Pyrolysis comprehensive two-dimensional gas chromatography study of petroleum source rock. Analytical Chemistry 79, 5642-5650.

Wilhelms, A., Larter, S.R.2004. Shaken but not always stirred. Impact of petroleum charge mixgin on reservoir geochemistry. In: J.M. Cubitt, W.A. England, S.R. Larter (Eds.), Understanding petroleum reservois: Towards an integrated reservoir engineering and geochemical approach. 237. (Ed. by J.M. Cubitt, W.A. England, S.R. Larter) Geological Society, London, pp. 27-35.

Zeng, H., Song, Y.-Q., Johnson, D.L., Mullins, O.C., 2009. Critical nanoaggregate concentration of asphaltenes by direct-current (DC) eletrical conductivity. Energy and Fuels 23, 1201-1208.

Zhan, D., Fenn, J.B., 2000. Electrospray mass spectrometry of fossil fuels. International Journal of Mass Spectrometry 194, 197-208.

Zumberge, J.E., 1987. Terpenoid biomarker distributions in low maturity crude oils. Organic Geochemistry 11, 479-496.